Genomics Data 2 (2014) 345–350

Contents lists available at ScienceDirect

Genomics Data

journal homepage: http://www.journals.elsevier.com/genomics-data/

Data in Brief

Microarray profiling to analyse adult cardiac fibroblast identity

Milena B. Furtado [a,*,1], Hieu T. Nim [a,b,*,1], Jodee A. Gould [c], Mauro W. Costa [a], Nadia A. Rosenthal [a,b,1], Sarah E. Boyd [a,b,1]

[a] Australian Regenerative Medicine Institute, Monash University, VIC 3800, Australia
[b] Systems Biology Institute (SBI) Australia, Monash University, VIC 3800, Australia
[c] Monash Health and Translational Precinct (MHTP), Medical Genomics Facility (MGF), VIC 3168, Australia

ARTICLE INFO

Article history:
Received 30 September 2014
Accepted 2 October 2014
Available online 12 October 2014

Keywords:
Microarray profiling
Heart fibroblast
Tail fibroblast
Open-source analysis

ABSTRACT

Heart failure is one of the leading causes of death worldwide [1–4]. Current therapeutic strategies are inefficient and cannot cure this chronic and debilitating condition [5]. Ultimately, heart transplants are required for patient survival, but donor organs are scarce in availability and only prolong the life-span of patients for a limited time. Fibrosis is one of the main pathological features of heart failure [6,7], caused by inappropriate stimulation of fibroblasts and excessive extracellular matrix production. Therefore, an in-depth understanding of the cardiac fibroblast is essential to underpin effective therapeutic treatments for heart failure [5]. Fibroblasts in general have been an underappreciated cell type, regarded as relatively inert and providing only basic functionality; they are usually referred to as the 'biological glue' of all tissues in the body. However, more recent literature suggests that they actively participate in organ homeostasis and disease [7,8].

We have recently uncovered a unique molecular identity for fibroblasts isolated from the heart [9], expressing a set of cardiogenic transcription factors that have been previously associated with cardiomyocyte ontogenesis. This signature suggests that cardiac fibroblasts may be ideal for use in stem cell replacement therapies, as they may retain the memory of where they derive from embryologically. Our data also revealed that about 90% of fibroblasts from both tail and heart origins share a cell surface signature that has previously been described for mesenchymal stem cells (MSCs), raising the possibility that fibroblasts and MSCs may in fact be the same cell type. Thus, our findings carry profound implications for the field of regenerative medicine. Here, we describe detailed methodology and quality controls related to the gene expression profiling of cardiac fibroblasts, deposited at the Gene Expression Omnibus (GEO) under the accession number GSE50531. We also provide the R code to easily reproduce the data quantification and analysis processes.

Specifications	
Organism/cell line/tissue	Mus musculus
Sex	Male
Sequencer or array type	Agilent SurePrint G3 mouse gene expression 8 × 60 k arrays
Data format	Raw and analysed
Experimental factors	Cultured tail and heart fibroblasts
Experimental features	Experiment comparing expression profile of mouse tail and cardiac fibroblasts in adult wild-type animals
Consent	All animal experimentation conformed with local (Monash University) and national guidelines in Australia, under breeding ethics license MARP/2011/038/BC and experimental license MARP/2011/175
Sample source location	Monash Animal Services (MAS), Melbourne, Australia (originally imported from The Jackson Laboratory, Maine, USA)

* Corresponding authors at: Australian Regenerative Medicine Institute, Monash University, VIC 3800, Australia.
[1] Both authors contributed equally to this work.

Direct link to deposited data

Deposited data can be found here: http://www.ncbi.nlm.nih.gov/geo/query/acc.cgi?acc=GSE50531.

Experimental design, materials and methods

Mouse usage

Eight-week old C57Bl/6J (http://jaxmice.jax.org/strain/000664.html) adult male mice were obtained from Monash Animal Services (MAS) facility, Monash University.

Fibroblast isolation and culture

Animals were humanely killed using CO_2 asphyxiation and hearts were perfused with 20 ml of Hank's Balanced Salt Solution without calcium or magnesium (HBSS-Gibco) using a 20 ml syringe and 26 gauge

http://dx.doi.org/10.1016/j.gdata.2014.10.006

needles. For perfusion, the needle was inserted into the left ventricular chamber, while the right atrial appendage was cut open to allow blood/buffer exit through the pulmonary circulation. This procedure removed excess blood from heart chambers. Prior to cell isolation, two wild-type mouse hearts per sample were finely minced using surgical scissors. Whole tails from the same animals were skinned and cut into 2–3 mm pieces. Both tissues were subjected to enzymatic digestion with 0.05% trypsin/EDTA (Gibco) at 37 °C under agitation for 40 min, washed in HBSS, cleared using 40 μm cell strainers for Falcon tubes (BD Biosciences) that retain undigested tissue, spun at 400 g for 5 min, resuspended in cell culture media [DMEM high glucose with glutamax (Gibco), supplemented with 10% foetal bovine serum (FBS-Gibco), 1× penicillin/streptomycin (Gibco) and 1× sodium pyruvate (Gibco)] and plated on 10 cm dishes (BD Biosciences). Next morning, plates were washed twice in phosphate buffered saline (PBS) without calcium or magnesium (Gibco) to remove debris. Media changes were performed every couple of days until day 5, after which cells were processed for RNA extraction. Cells were cultured in a humidified incubator with 5% CO_2 at 37 °C.

RNA preparation

Cultured fibroblasts from heart and tail were processed for total RNA extraction using the mirVana kit (Ambion) as per manufacturer's instructions. Briefly, 10 cm dishes containing heart or tail fibroblasts were washed twice in PBS (Gibco) and 500 μl of RNA lysis solution was added to dishes. Cell scrapers (BD Biosciences) were used to homogenise cell disruption, after which 1:10 (v/v) of miRNA homogenate additive was added. Samples were subjected to organic extraction using acid phenol:chloroform and 1.25 volume of ethanol was added to aqueous phases, which were passed through a filter cartridge, washed in kit wash solutions 1 and 2 and eluted in 50 μl of pre-heated (95 °C) elution solution. Following manufacturer's recommendations for total RNA recovery, we have not enriched samples for small RNAs. All samples

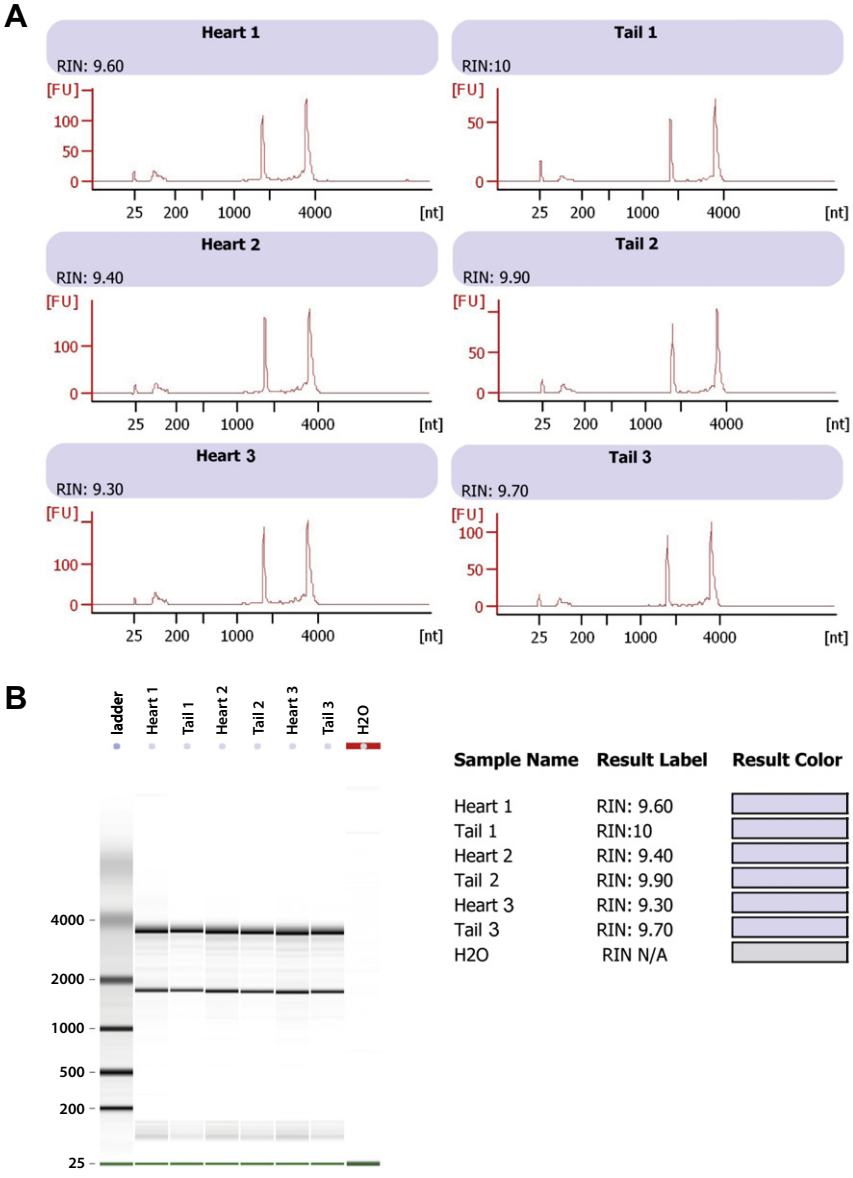

Fig. 1. Quality control (QC) analysis for samples used for microarray. A. Electropherogram shows typical plot for high quality total RNA, peaks for 18 s and 28 s ribosomal RNA subunits can be clearly seen for all samples and no intermediate peaks, equivalent to degradation products, are observed. B. Gel image showing expected migration pattern for intact RNA on tail and heart samples, highlighting 18 s (below 2000 bp band of ladder) and 28 s (below 4000 bp band of ladder) ribosomal RNA. Small peaks 25 and 200 nucleotides correspond to the loading marker and small RNAs, respectively. RNA Integrity Number (RIN) scores vary from a minimum of 0 (degraded) to a maximum of 10 (intact) total RNA. nt — nucleotide; FU — fluorescence intensity.

were DNAse digested using DNAseI from the DNA-free kit (Ambion) for 20 min at 37 °C, after which 1:10 (v/v) DNAse inactivation reagent was added, mixed for 2 min at room temperature and spun down at maximum speed for 90 s in an Eppendorf centrifuge to pellet inactivation beads. Samples were transferred into clean tubes and further processed at the Medical Genomics Facility.

Microarray study design

Three replicate samples were profiled per condition (i.e. heart or tail fibroblasts).

RNA labelling and hybridization

Total RNA from 6 samples (3 tail and 3 heart replicas) was used for microarray analysis. All samples showed RNA integrity numbers (RINs) ranging between 9–10, as determined by the 2100 Bioanalyser (Agilent) (Fig. 1). 0.1 μg of total RNA was used to prepare Cyanine-3 (Cy3) labelled cRNA for hybridization. For labelling, the One-Color Low input Quick Amp labelling Kit (Agilent) was used according to the manufacturer's instructions, after which labelled RNA was cleaned using by RNeasy column purification (Qiagen). Dye incorporation and cRNA yield were determined with the NanoDrop ND-1000 Spectrophotometer.

For chip hybridization, 600 ng of Cy3 labelled cRNAs were fragmented at 60 °C for 30 min in a reaction volume of 25 μl containing 1× Agilent Fragmentation buffer and 2× Agilent Gene Expression Blocking agent. Specific activities ranging between 16–18 pmol Cy3/μg cRNA were used for each sample. On completion, 25 μl of 2× HI-RPM Gene Expression buffer (Agilent) was added. 40 μl of samples were hybridised on SurePrint G3 Mouse GE 8 × 60 K microarrays (Agilent) for 17 h at 65 °C in a rotating hybridisation oven (Agilent). Following hybridisation, microarrays were washed with GE wash buffer 1 (Agilent) for 1 min at room temperature and with GE wash buffer 2 at 37 °C for 1 min. Microarrays were scanned with an Agilent C, DNA microarray scanner at 3 μm resolution (scan area 61 × 21.6 mm), dye channel set to green, 20 bit tiff. The scanned images were analysed with Agilent Feature Extraction Software 11.0.1.1 to obtain background subtracted and spatially detrended Processed Signal intensities.

Data normalisation and analysis

Samples were processed by the Monash Health Translation Precinct (MHTP) Medical Genomics Facility, and run on Agilent SurePrint G3 mouse gene expression arrays (single colour), followed by analysis with GeneSpring 12.6, using quantile normalisation with no baseline transformation, logbase 2. Unpaired T test ($p <= 0.05$, $logFC >= 2.0$) with Benjamini–Hochberg correction was used to find differentially

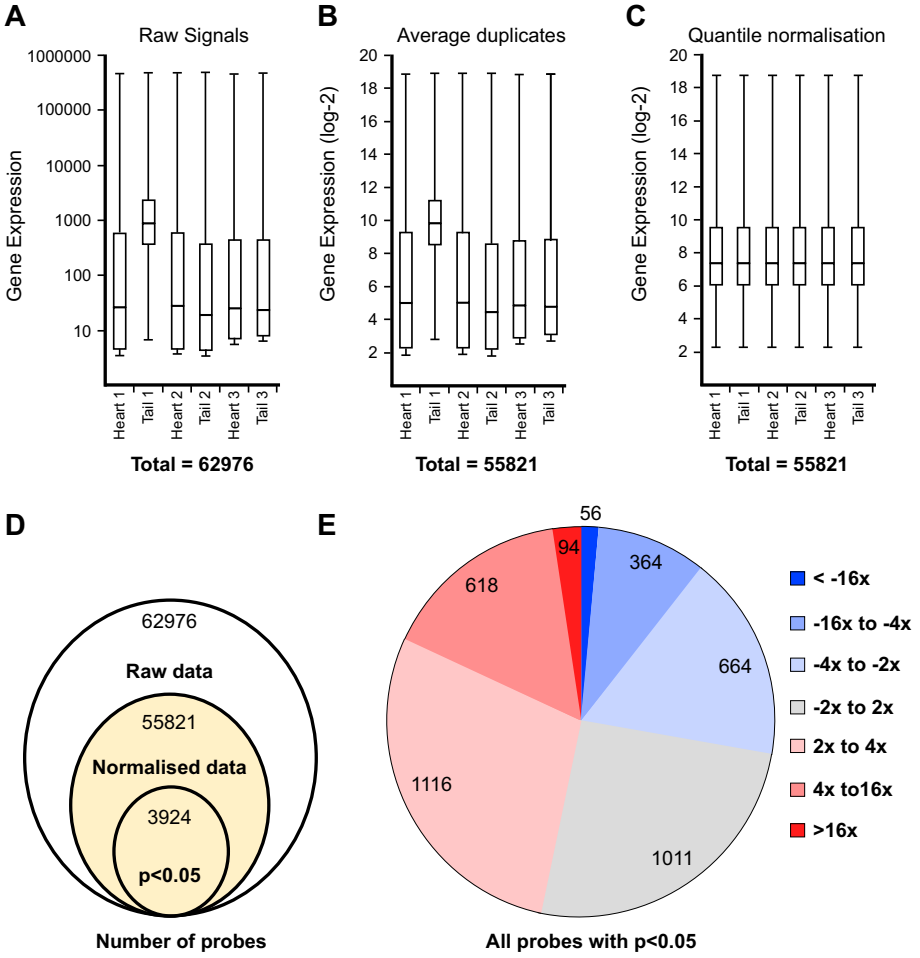

Fig. 2. Normalisation and transcriptome-wide comparison between cardiac fibroblasts and tail fibroblasts. (A–C) Box-plots of the gene expression data at the end of each pre-processing and normalisation processing stage: (A) Single-channel signals extracted from Agilent Feature Extraction Software; (B) data pre-processing, duplicates averaging and log-2 transformation; and (C) quantile normalisation. After normalisation, all samples have identical distributions. (D) Venn diagram illustrating the initial number of entities in the raw data (62,976 genes), the reduction of data points through processing and normalisation (55,821 genes), and finally the pool of differentially-expressed entities with p-value < 0.05 (3924 genes). (E) Distribution of the level of gene expression fold-changes within the pool of 3924 differentially-expressed entities.

expressed genes. These results have been reported in the original article [9].

For the purpose of improved accessibility, a similar analysis was performed here using an open-source pipeline with R and Bioconductor. The raw single-channel signals were extracted with Agilent Feature Extraction Software 11.0.1.1. Non-uniform, saturated probes, and population outliers were filtered using the default "Compromised" option in GeneSpring GX12.6 (Agilent), with threshold raw signal of 1.0. At the end of this process, 6 text files (.txt) were exported for the data normalisation stage. This analysis has been deposited in GEO under the accession number (to be allocated by GEO) and is linked to the original samples GSM1220786-91 under accession number GSE50531.

Data normalisation was performed with R (http://www.r-project.org) using the publicly available Bioconductor packages (bioconductor.org) [10]. Three pre-processing and normalisation steps were performed: (1) use *read.maimage* function to extract the *gProcesedSignal* values from the GeneSpring exported data files (Fig. 2A); (2) use *avereps.EList* function to average the duplicate spots and log-2 transformation (Fig. 2B); and (3) use *normalizeBetweenArrays* function to perform quantile normalisation on all arrays (Fig. 2C).

Differential analysis between cardiac fibroblast and tail fibroblast samples was performed using the Bioconductor limma package [11], which applies linear models and differential expression functions to the transcriptomic data. With 6 normalised arrays having identical distributions (Fig. 2C), the *lmFit* function identifies the genes that have differential expression between 3 cardiac fibroblast samples and 3 tail fibroblast samples. At a p-value threshold of 0.05, we identified a pool of 3924 differentially expressed entities (Fig. 2D). These entities were used for fold-change calculation (Fig. 2E), revealing 94 strongly up-regulated entities (16×) and 56 strongly down-regulated entities (−16×). Tables 1.1 and 1.2 detailed the gene symbols corresponding to the strongly up- and down-regulated entities, which revealed many cardiogenic genes, including *Tcf21*, *Tbx20* and *Gata4*. The R code to reproduce this analysis is available in GEO.

Discussion

Our goal for the current experiment was to identify cardiac fibroblast-specific genes [1-8]. For this purpose, isolated cells were cultured for 5 days in order to remove carry-over of debris and DNA/RNA from dead

Table 1.1
List of differentially expressed entities when comparing cardiac fibroblasts to tail fibroblasts (up-regulated, fold change > 16×, p < 0.05).

Probe 1 0	Gene symbol	Log fold change	p-Value	Probe 1 0	Gene symbol	Log fold change	p-Value
A_51_P459944	Tcf21	7.774715027	1.38E-07	A_51_P215475	Ptprb	4.720490634	0.00037027
A_51_P255699	Mmp3	7.668280653	1.93E-05	A_52_P145415	Ptch2	4.695570013	5.40E-06
A_55_P1982291	Clcal	7.533997026	0.00012796	A_66_P136813	6030408B16R	4.683599203	0.00010558
A_52_P58145	Aldh1a2	7.293188199	2.35E-07	A_55_P1982404	Gpm6b	4.641949565	0.00142493
A_51_P265806	Clca2	7.201895798	3.98E-05	A_55_P2108012	Fam78b	4.616958484	6.96E-05
A_52_P429876	Tbx20	7.199004006	1.04E-06	A_55_P1962305	Plac8	4.595679816	0.00118151
A_52_P579531	Pdlim3	6.798017108	3.01E-06	A_52_P266132	Fgl2	4.584599456	0.00088425
A_55_P2111302	Cp	6.728089433	1.49E-06	A_55_P2088720		4.54706191	2.21E-05
A_51_P419637	Dclk3	6.63184125	1.94E-07	A_55_P2109585	Plekha7	4.539532165	1.74E-06
A_55_P2017418	Cfh	6.541868044	4.38E-05	A_55_P2102769	Abca8a	4.535543021	0.00205118
A_55_P2028894	Gata4	6.490939109	9.05E-05	A_55_P2007495		4.513579208	4.12E-05
A_55_P2108248	Art4	6.471910595	0.00010405	A_55_P2029746		4.492855257	1.38E-05
A_51_P110301	C3	6.32871005	0.00039752	A_55_P2051596		4.477946264	0.0002982
A_55_P1970385		6.286227697	3.22E-05	A_51_P468140	Serpind1	4.47050946	0.00126139
A_52_P614777	Sucnr1	6.074222864	0.00026042	A_51_P301998	Fmo2	4.458776979	6.63E-06
A_55_P2162503	Tbx20	6.001391067	0.00017203	A_55_P1974845	Pde1a	4.457633544	3.85E-06
A_55_P1992049	Gucy1a3	5.982102699	0.00028777	A_55_P2169356		4.456953685	0.00467752
A_51_P127297	Hsd11b1	5.953520453	5.85E-07	A_55_P1953846	Abca8b	4.450698252	0.00092446
A_51_P159453	Serpina3n	5.799342267	0.00145534	A_55_P1954724	Gm20186	4.412602719	1.39E-05
A_52_P28960	Gdf6	5.688645717	1.73E-06	A_55_P2153783	Fmo1	4.408916363	2.90E-06
A_55_P2036240		5.673154478	4.05E-05	A_52_P179068	Gucy1b3	4.403895518	0.00191671
A_51_P286748	Frzb	5.607110137	4.68E-05	A_55_P1957213	3930401B19R	4.398861887	1.74E-05
A_51_P116651	Opt	5.603519237	0.00067503	A_55_P2026270	Cfi	4.390561823	0.00108725
A_55_P2054854	Art4	5.570955142	0.00336205	A_55_P2140212		4.366229602	2.05E-05
A_55_P2038525	C3	5.499803595	5.12E-05	A_55_P2017347	Krtap11–1	4.326344638	0.00387402
A_55_P2124461		5.433866138	3.25E-06	A_55_P2114318		4.31693497	2.77E-05
A_51_P376445	Rhox5	5.334853046	0.00452163	A_55_P2026547	Gal3st2	4.287884906	0.0001618
A_55_P2059010	Rbp1	5.268991948	2.76E-06	A_55_P2162910	Rtn1	4.277702379	0.00013212
A_55_P2159485		5.254034014	0.00084844	A_51_P501248	Sphk1	4.239981128	6.43E-05
A_55_P1996973	Gvi n1	5.219003996	0.00589851	A_51_P173709	Gprc5b	4.216740223	0.00086867
A_30_P01023737		5.208384457	1.18E-05	A_52_P535484	Gvin1	4.2100439	0.00072863
A_55_P2071952	Wdr92	5.164057614	1.34E-05	A_55_P2430367	Zbtb8b	4.180203889	4.91E-06
A_51_P367780	Adamts12	5.153752038	2.08E-05	A_51_P441426	Pf4	4.177619023	0.00022135
A_52_P120803	Ankrd1	5.150091794	0.00061576	A_30_P01020754		4.169537934	5.55E-05
A_52_P220879	Tgm2	5.097421217	0.00035587	A_51_P503625	Gsta3	4.15056312	0.00017442
A_55_P2185890	Cfh	5.058590753	1.54E-05	A_51_P264695	Crym	4.124721129	0.00368514
A_55_P1984655	5mtnl2	5.048007589	0.00066022	A_55_P2048855	Sprr2a2	4.10440044	7.57E-06
A_51_P508838	Kcne4	5.041911898	4.91E-06	A_52_P337259	Heyl	4.0902626	6.83E-06
A_55_P2107785		5.02223357	4.56E-05	A_55_P1983858	Seel	4.076340425	1.99E-05
A_52_P381484	Spon2	4.995680379	1.40E-06	A_55_P1963463	Gabra3	4.060184936	0.00456924
A_55_P2017413	Gm4788	4.974910672	4.43E-05	A_55_P1958165	Ms4a7	4.059035938	3.70E-05
A_55_P1964960	IL13	4.957875799	0.00183759	A_55_P2099742	Ccl19	4.034638511	0.00020569
A_51_P334942	Aldh1a1	4.930168491	9.06E-07	A_55_P2016237	Hand2	4.024649163	1.76E-06
A_51_P153423	Fndc1	4.924289787	4.64E-05	A_52_P472302	Fxyd6	4.021862402	5.70E-06
A_51_P335460	Scin	4.921316898	3.03E-06	A_51_P176352	Ndrg2	4.002251368	0.00037256
A_55_P2007496		4.888471012	0.00065309				
A_52_P796840	Cfhr2	4.807319461	7.84E-06				
A_51_P246166	Wfdc18	4.794125063	0.00010262				
A_55_P1998811		4.74419517	6.38E-05				

Table 1.2
List of differentially expressed entities when comparing cardiac fibroblasts and tail fibroblasts (down-regulated, fold change <−16×, p < 0.05).

Probe ID	Gene symbol	Log fold change	p-Value
A_52_P401504	Thbs4	−9.592174841	1.22E-07
A_55_P2163033	Hoxb13	−9.413716631	4.47E-07
A_51_P152990	Grem2	−8.848601783	2.76E-08
A_51_P241068	Dkk2	−7.605061419	1.48E-06
A_30_P01024322		−6.845383532	0.00167504
A_51_P339793	111rl1	−6.624788912	2.97E-06
A_30_P01022821		−6.236747352	8.13E-05
A_55_P1977431	Cck	−6.210979682	2.50E-05
A_55_P2380806	Gm2115	−6.047107571	1.49E-06
A_55_P1983754	Pcp411	−6.022954787	5.01E-06
A_52_P1092823	Irx1	−5.709918806	7.44E-07
A_30_P01017882		−5.589314885	3.33E-05
A_55_P2125311	Rab3b	−5.524900093	5.71E-07
A_55_P2104219	Hoxc13	−5.350209094	1.25E-06
A_30_P01030354		−5.247161242	0.01040968
A_55_P1963807	Actg2	−5.05268315	1.23E-06
A_55_P1959633	Hnf4a	−5.01046471	0.0084615
A_51_P431329	Car3	−4.999183138	0.00029175
A_55_P2275437		−4.971382946	0.0001802
A_51_P254425	Ah rr	−4.931766401	1.13E-06
A_51_P453909	Cyp2f2	−4.90093426	1.07E-05
A_52_P547612	Tmem30b	−4.882588964	3.74E-06
A_55_P1970075	Hoxa13	−4.838619293	1.99E-06
A_30_P01023831		−4.836691283	1.42E-06
A_55_P2035946	Penk	−4.821628549	4.05E-06
A_51_P112223	Gsta4	−4.793332842	1.64E-06
A_51_P350817	Cnn1	−4.788691188	1.87E-06
A_30_P01027398		−4.776324333	8.12E-05
A_55_P2126192	Lgr5	−4.678393687	0.00126788
A_51_P309488	1810058N15Ril	−4.676510147	3.09E-06
A_51_P253481	Ces1g	−4.633576905	0.00024964
A_30_P01019159		−4.60457949	3.24E-05
A_52_P374960	Ostn	−4.570737399	0.00132575
A_51_P222337	Rspo2	−4.566245563	0.00010263
A_55_P1984896	Fsip2	−4.54577185	0.00054826
A_55_P2028399	Hoxc11	−4.466924796	3.41E-05
A_55_P2107140	Olfr323	−4.46213166	6.91E-05
A_52_P973575	Hoxb9	−4.442393871	4.66E-05
A_51_P176202	Ankrd36	−4.369381912	0.00103598
A_52_P569375	Fgf5	−4.365217026	0.00794978
A_51_P108183	Tnmd	−4.345146004	0.00198834
A_51_P194230	Zic1	−4.320743819	3.29E-05
A_51_P241319	Cilp	−4.272317182	0.00206339
A_51_P413111	Ppm1l	−4.265754405	3.35E-06
A_51_P215374	Slc6a17	−4.220019679	0.00027602
A_55_P2163659	Rspo3	−4.177589527	0.00011669
A_51_P375754	Hoxc10	−4.165266321	0.00468582
A_55_P2103297		−4.153975645	4.06E-06
A_55_P2001486		−4.137007991	7.49E-05
A_52_P194971	Hoxb7	−4.093762326	0.00026535
A_55_P2360800	C230060E24	−4.071029277	0.00301094
A_51_P516637	Bmp5	−4.058261531	0.00185459
A_55_P2069226		−4.0448526	0.000832
A_55_P2053933	Foxa1	−4.04379596	7.51E-05
A_55_P2014249	Sema3a	−4.042700618	0.00119229
A_52_P337126	Bves	−4.006299	0.00071079

cardiomyocytes present in fresh preparations. Contamination with cardiomyocyte structural markers has been reported in previous analyses [12], as the cell isolation method for compact tissue requires harsh enzymatic dissociation conditions, which causes extensive cardiomyocyte death. We found that a 5-day passage 0 culture produces non-confluent, highly healthy cells where no statistically significant contamination with cardiomyocyte genes can be detected.

Upon visualisation of the raw data (Fig. 2A), we noticed that sample Tail2 showed higher overall signal intensity than others. As all samples were processed simultaneously and showed similar RIN scores (Fig. 1), we believe this finding is a technical problem inherent to the hybridization step or chip composition. Nevertheless, this discrepancy did not impair our analysis.

As with many microarray datasets, data noise is an important issue. We performed differential analysis using the robust *lmFit* method, which is widely regarded as noise-tolerant in the bioinformatics community. The high-confidence entities evaluated by log fold-change and p-value (such as the cardiogenic genes *Tcf21* and *Tbx20*) were subsequently validated using qPCR validation to confirm their biological relevance, as described by our main research article [9].

The microarray analysis pipeline described here made use of both the proprietary GeneSpring GX12.6 software and open source R packages. In addition to our original analysis [9], we have provided a second open-source analysis to facilitate the reproducibility of our study. Due to differences between methods (algorithms) provided by limma and GeneSpring, and the closed-nature of the Genespring software, there are discrepancies between the final fold-change calculations between the two analyses. However, although the exact values differed for entities found up- and down-regulated in the open source analysis, our genes of interest were similarly differentially regulated in both analyses.

A range of bona fide haematopoietic genes were up-regulated in heart samples, for example *Ccl19*, *Cd28*, *Mpeg1*, *Plac8* and *Cx3cr1*, while other haematopoietic markers, such as *Cd45*, *Cd31 and Cd34* were not significantly altered. Most of these genes have not been correlated with fibroblast biology yet, although expression of *Cx3cr1* has been previously reported in cardiac fibroblasts [13]. We have also not detected significant levels of CD31, CD34 or CD45 protein in our samples [9], supporting the argument that if present, haematopoietic cells are not a major contaminant in our cultures. However, leukocyte contamination in our cultures cannot be ruled out at this point. As our laboratory has previously characterised a population of resident macrophages in the heart [12], follow-up experiments using sorted $CD90^{+}$, $CD45^{+}$, $CD31^{-}$ cells would clarify this issue.

Conflict of interest

The authors have no conflict of interest.

Funding

The ARC Discovery Grant DP130104792 was given to SEB and HK; and The ARC Stem Cell Grant and NHMRC Australia Fellowship were given to NR. The Australian Regenerative Medicine Institute is supported by grants from the State Government of Victoria and the Australian Government.

Acknowledgements

We acknowledge the use of facilities Monash Animal Services (MAS) and MHTP Medical Genomics Facility.

Appendix A. Supplementary data

Supplementary data to this article can be found online at http://dx.doi.org/10.1016/j.gdata.2014.10.006.

References

[1] A.S. Go, D. Mozaffarian, V.L. Roger, E.J. Benjamin, J.D. Berry, M.J. Blaha, S. Dai, E.S. Ford, C.S. Fox, S. Franco, H.J. Fullerton, C. Gillespie, S.M. Hailpern, J.A. Heit, V.J. Howard, M.D. Huffman, S.E. Judd, B.M. Kissela, S.J. Kittner, D.T. Lackland, J.H. Lichtman, L.D. Lisabeth, R.H. Mackey, D.J. Magid, G.M. Marcus, A. Marelli, D.B. Matchar, D.K. McGuire, E.R. Mohler III, C.S. Moy, M.E. Mussolino, R.W. Neumar, G. Nichol, D.K. Pandey, N.P. Paynter, M.J. Reeves, P.D. Sorlie, J. Stein, A. Towfighi, T.N. Turan, S.S. Virani, N.D. Wong, D. Woo, M.B. Turner, American Heart Association Statistics C, Stroke Statistics S. Executive summary: heart disease and stroke statistics-2014 update: a report from the American Heart Association. Circulation 129 (2014) 399–410.

[2] A.S. Go, D. Mozaffarian, V.L. Roger, E.J. Benjamin, J.D. Berry, M.J. Blaha, S. Dai, E.S. Ford, C.S. Fox, S. Franco, H.J. Fullerton, C. Gillespie, S.M. Hailpern, J.A. Heit, V.J. Howard, M.D. Huffman, S.E. Judd, B.M. Kissela, S.J. Kittner, D.T. Lackland, J.H. Lichtman, L.D. Lisabeth, R.H. Mackey, D.J. Magid, G.M. Marcus, A. Marelli, D.B.

Matchar, D.K. McGuire, E.R. Mohler III, C.S. Moy, M.E. Mussolino, R.W. Neumar, G. Nichol, D.K. Pandey, N.P. Paynter, M.J. Reeves, P.D. Sorlie, J. Stein, A. Towfighi, T.N. Turan, S.S. Virani, N.D. Wong, D. Woo, M.B. Turner, American Heart Association Statistics C, Stroke Statistics S. Heart disease and Stroke Statistics-2014 update: a report from the American Heart Association. Circulation 129 (2014) e28–e292.

[3] S.S. Lim, T. Vos, A.D. Flaxman, G. Danaei, K. Shibuya, H. Adair-Rohani, M. Amann, H.R. Anderson, K.G. Andrews, M. Aryee, C. Atkinson, L.J. Bacchus, A.N. Bahalim, K. Balakrishnan, J. Balmes, S. Barker-Collo, A. Baxter, M.L. Bell, J.D. Blore, F. Blyth, C. Bonner, G. Borges, R. Bourne, M. Boussinesq, M. Brauer, P. Brooks, N.G. Bruce, B. Brunekreef, C. Bryan-Hancock, C. Bucello, R. Buchbinder, F. Bull, R.T. Burnett, T.E. Byers, B. Calabria, J. Carapetis, E. Carnahan, Z. Chafe, F. Charlson, H. Chen, J.S. Chen, A.T. Cheng, J.C. Child, A. Cohen, K.E. Colson, B.C. Cowie, S. Darby, S. Darling, A. Davis, L. Degenhardt, F. Dentener, D.C. Des Jarlais, K. Devries, M. Dherani, E.L. Ding, E.R. Dorsey, T. Driscoll, K. Edmond, S.E. Ali, R.E. Engell, P.J. Erwin, S. Fahimi, G. Falder, F. Farzadfar, A. Ferrari, M.M. Finucane, S. Flaxman, F.G. Fowkes, G. Freedman, M.K. Freeman, E. Gakidou, S. Ghosh, E. Giovannucci, G. Gmel, K. Graham, R. Grainger, B. Grant, D. Gunnell, H.R. Gutierrez, W. Hall, H.W. Hoek, A. Hogan, H.D. Hosgood III, D. Hoy, H. Hu, B.J. Hubbell, S.J. Hutchings, S.E. Ibeanusi, G.L. Jacklyn, R. Jasrasaria, J.B. Jonas, H. Kan, J.A. Kanis, N. Kassebaum, N. Kawakami, Y.H. Khang, S. Khatibzadeh, J.P. Khoo, C. Kok, F. Laden, R. Lalloo, Q. Lan, T. Lathlean, J.L. Leasher, J. Leigh, Y. Li, J.K. Lin, S.E. Lipshultz, S. London, R. Lozano, Y. Lu, J. Mak, R. Malekzadeh, L. Mallinger, W. Marcenes, L. March, R. Marks, R. Martin, P. McGale, J. McGrath, S. Mehta, G.A. Mensah, T.R. Merriman, R. Micha, C. Michaud, V. Mishra, K. Mohd Hanafiah, A.A. Mokdad, L. Morawska, D. Mozaffarian, T. Murphy, M. Naghavi, B. Neal, P.K. Nelson, J.M. Nolla, R. Norman, C. Olives, S.B. Omer, J. Orchard, R. Osborne, B. Ostro, A. Page, K.D. Pandey, C.D. Parry, E. Passmore, J. Patra, N. Pearce, P.M. Pelizzari, M. Petzold, M.R. Phillips, D. Pope, C.A. Pope III, J. Powles, M. Rao, H. Razavi, E.A. Rehfuess, J.T. Rehm, B. Ritz, F.P. Rivara, T. Roberts, C. Robinson, J.A. Rodriguez-Portales, I. Romieu, R. Room, L.C. Rosenfeld, A. Roy, L. Rushton, J.A. Salomon, U. Sampson, L. Sanchez-Riera, E. Sanman, A. Sapkota, S. Seedat, P. Shi, K. Shield, R. Shivakoti, G.M. Singh, D.A. Sleet, E. Smith, K.R. Smith, N.J. Stapelberg, K. Steenland, H. Stockl, L.J. Stovner, K. Straif, L. Straney, G.D. Thurston, J.H. Tran, R. Van Dingenen, A. van Donkelaar, J.L. Veerman, L. Vijayakumar, R. Weintraub, M.M. Weissman, R.A. White, H. Whiteford, S.T. Wiersma, J.D. Wilkinson, H.C. Williams, W. Williams, N. Wilson, A.D. Woolf, P. Yip, J.M. Zielinski, A.D. Lopez, C.J. Murray, M. Ezzati, M.A. AlMazroa, Z.A. Memish, A comparative risk assessment of burden of disease and injury attributable to 67 risk factors and risk factor clusters in 21 regions, 1990–2010: a systematic analysis for the global burden of disease study 2010. Lancet 380 (2012) 2224–2260.

[4] C.D. Mathers, D. Loncar, Projections of global mortality and burden of disease from 2002 to 2030. PLoS Med. 3 (2006) e442.

[5] E.B. Schelbert, G.C. Fonarow, R.O. Bonow, J. Butler, M. Gheorghiade, Therapeutic targets in heart failure: refocusing on the myocardial interstitium. J. Am. Coll. Cardiol. 63 (2014) 2188–2198.

[6] K.B. Schuetze, T.A. McKinsey, C.S. Long, Targeting cardiac fibroblasts to treat fibrosis of the heart: focus on hdacs. J. Mol. Cell. Cardiol. 70 (2014) 100–107.

[7] S. Van Linthout, K. Miteva, C. Tschope, Crosstalk between fibroblasts and inflammatory cells. Cardiovasc. Res. 102 (2014) 258–269.

[8] T. Moore-Morris, N. Guimaraes-Camboa, I. Banerjee, A.C. Zambon, T. Kisseleva, A. Velayoudon, W.B. Stallcup, Y. Gu, N.D. Dalton, M. Cedenilla, R. Gomez-Amaro, B. Zhou, D.A. Brenner, K.L. Peterson, J. Chen, S.M. Evans, Resident fibroblast lineages mediate pressure overload-induced cardiac fibrosis. J. Clin. Invest. 124 (2014) 2921–2934.

[9] M.B. Furtado, M.W. Costa, E.A. Pranoto, E. Salimova, A.R. Pinto, N.T. Lam, A. Park, P. Snider, A. Chandran, R.P. Harvey, R. Boyd, S.J. Conway, J. Pearson, D.M. Kaye, N.A. Rosenthal, Cardiogenic genes expressed in cardiac fibroblasts contribute to heart development and repair. Circ. Res. 114 (2014) 1422–1434.

[10] R.C. Gentleman, V.J. Carey, D.M. Bates, B. Bolstad, M. Dettling, S. Dudoit, B. Ellis, L. Gautier, Y. Ge, J. Gentry, K. Hornik, T. Hothorn, W. Huber, S. Iacus, R. Irizarry, F. Leisch, C. Li, M. Maechler, A.J. Rossini, G. Sawitzki, C. Smith, G. Smyth, L. Tierney, J.Y. Yang, J. Zhang, Bioconductor: open software development for computational biology and bioinformatics. Genome Biol. 5 (2004) R80.

[11] G.K. Smyth, Limma: linear models for microarray data. in: R. Gentleman, V. Carey, W. Huber, R. Irizarry, S. Dudoit (Eds.), Bioinformatics and Computational Biology Solutions Using r and Bioconductor, Elsevier, New York, 2005, pp. 397–420.

[12] A.R. Pinto, R. Paolicelli, E. Salimova, J. Gospocic, E. Slonimsky, D. Bilbao-Cortes, J.W. Godwin, N.A. Rosenthal, An abundant tissue macrophage population in the adult murine heart with a distinct alternatively-activated macrophage profile. PLoS ONE 7 (2012) e36814.

[13] W. Xuan, Y. Liao, B. Chen, Q. Huang, D. Xu, Y. Liu, J. Bin, M. Kitakaze, Detrimental effect of fractalkine on myocardial ischaemia and heart failure. Cardiovasc. Res. 92 (2011) 385–393.